Flow Separation over Axisymmetric Afterbody Models

Walter M. Presz Jr.*
Pratt & Whitney Aircraft, East Hartford, Conn.
and
Edward T. Pitkin†
University of Connecticut, Storrs, Conn.

Separated flow data for axisymmetric afterbodies are presented. A number of models were tested at subsonic Mach numbers through a range of unseparated, partially separated, and totally separated flow. The separation and reattachment locations on the afterbody were determined by oil flow visualization techniques, and static pressure taps were used to determine the surface pressure distribution in the separated region. The data systematically show the effect of shape, Mach number, total pressure and approach boundary-layer thickness upon the onset and extent of flow separation over afterbody models. Existing separation criteria are compared to the data; and an engineering model is proposed for use in predicting the effects of the separated region upon afterbody pressure distribution.

Introduction

THE problem of turbulent boundary-layer flow separation remains one of the fundamental problems of aerodynamics and is a phenomenon of critical importance to the design and performance of aircraft. Flow separation is encountered in many areas on an aircraft including the aft end and/or jet engine external afterbody. The separation is a result of the large adverse pressure gradients and the thick boundary layers that exist in these areas, and usually results in increased drag.

At present, there are no truly satisfactory methods for predicting and modeling separation. Furthermore, a lack of useful experimental data has limited the development of both analytical and empirical techniques in this area. Some experimental results on two-dimensional wing profiles and on two-dimensional steps are available but generally data are scarce, especially over axisymmetric contours. Considerably more data are required in order to evaluate the available methods of prediction and to improve or develop new methods. For this reason a detailed experimental test program was conducted at the Univ. of Connecticut to study flow separation over axisymmetric afterbody models. The results of this test program, containing new and useful information on flow separation, are the basis for this paper.

Experimental Equipment

The testing was done on 2 in. diam axisymmetric models in a 6 in. × 6 in. × 10 in. blow down wind tunnel. Total pressure was maintained by a pneumatically controlled throttle valve actuated by a feedback control loop which sensed test section total pressure. Limited Reynolds number variation was possible through adjustment of the total pressure. The models were tested at three Mach numbers, 0.25, 0.50, and 0.70, and at three total pressures, 30, 45, and 60 psia.

The models, shown schematically in Fig. 1 were sting mounted and made in three sections which could be combined into 18 different contour lengths and shapes. All were designed so that separation would occur on the afterbody section. The various length midsections were used to vary the thickness of the boundary layer approaching the afterbody sections, and a total pressure rake was used to measure this thickness. The various afterbody contours were designed with three general meridinal profiles; circular arc, conical and elliptical, in an effort to determine pressure gradient effects on separation. Each of these contours was further varied by changing its mean slope, thus altering the extent and depth of the separation region occurring on the models. Approximately 48 pressure taps (thirty on the afterbody section) were used to determine the pressure distribution in the separated flow region. The pressure measurements were made using a rapid switching Scanivalve commutator which selects from various pressure inputs and delivers a like output to a transducer for conversion to an electrical signal. The 48 individual pressures were recorded this way in five seconds of run time. The entire pressure-measurement system had an accuracy of ±0.005 psi.

After a variety of preliminary flow visualization experiments the points of separation and reattachment on the afterbody models were measured using an oil film technique. A multiviscosity motor oil mixed with lampblack paste worked well as shown in Fig. 2, which is a typical photograph obtained using this technique. The attached flow is readily recognized by the uniform pattern present

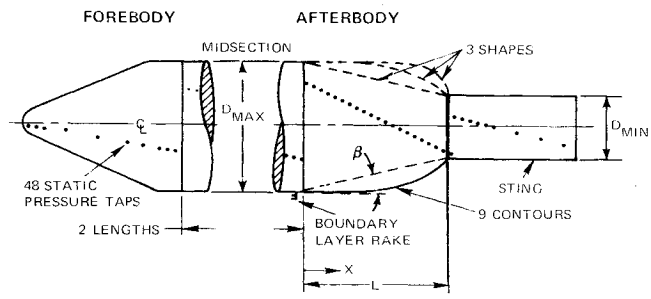

Fig. 1 Experimental models.

Presented as Paper 74-17 at the AIAA 12th Aerospace Sciences Meeting, Washington, D.C., January 30–February 1, 1974; submitted February 5, 1974; revision received June 6, 1974. The computational part of this work was performed in the computer center of the University of Connecticut, which is supported in part by Grant GJ-9 of the National Science Foundation.

Index categories: Aircraft Aerodynamics (Including Component Aerodynamics); Jets, Wakes, and Viscid-Inviscid Flow Interactions; Airbreathing Propulsion, Subsonic and Supersonic.

*Assistant Project Engineer, Propulsion Integration Group. Associate Member AIAA.

†Professor of Mechanical and Aerospace Engineering. Associate Fellow AIAA.

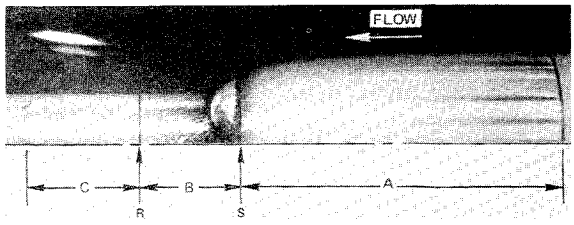

Fig. 2 Flow visualization technique.

in regions A and C. At separation wall skin friction approaches zero, and the oil mixture builds up as seen by the dark section between regions A and B. This dark section is followed by an oil streak pattern in region B which indicates a separated recirculating flow area. The oil pattern becomes orderly again once the flow reattaches on the downstream sting. Lines were used on the original polaroid photograph to document the location of separation and reattachment. These lines are evident in Fig. 2 and should not be confused with the oil film.

Experimental Results

Existing data and analysis suggest that afterbody flow separation is primarily a function of afterbody shape, freestream Mach number, freestream Reynolds number, and the approach boundary-layer characteristics. This section presents measured effects of these four variables on the separation over an afterbody.

Separation is a result of an adverse pressure gradient causing reverse flow of the low-energy low-momentum fluid in the boundary layer. The adverse pressure gradient occurring on an afterbody is determined by the inviscid flowfield and thus, the afterbody shape. When the freestream Mach number is greater than 0.2, compressibility effects can steepen the pressure gradients significantly. Approach boundary-layer thickness and velocity profile are critical since they define the energy and momentum of the fluid in the boundary layer and ultimately the pressure rise that can be tolerated without flow reversal near the boundaries. Reynolds number, representing the ratio of inertial to viscous forces in the flowfield, is an indication of the momentum transfer effect upon the separation process. At higher Reynolds numbers more momentum is transferred to the boundary-layer, and thus steeper pressure gradients can be imposed upon the boundary layer before separation.

Figure 3 presents the effects of varying freestream Mach number, M, on separation and pressure distributions over a 16° mean angle, β, circular arc afterbody. These curves show the measured pressure distributions in terms of pressure coefficients, C_p, over the model at freestream Mach numbers of 0.25, 0.50, and 0.70 where

$$C_p = [2(P - P_\infty)/kP_\infty M^2]$$

P_∞ is the freestream pressure and k is the ratio of specific heats. The points of separation, S, and reattachment, R, are determined by oil streak photography. It can be seen that the location of the separation point moves upstream and the reattachment point moves downstream with increasing Mach number. This separation point movement was evident on all the models tested and is consistent with Chang's[1] analytical results which show earlier separation to accompany compressibility effects. Even though the flow separates sooner and the separation region increases in size with Mach number, the C_p change between the point of maximum expansion and the point of separation tends to increase slightly with Mach number. The separated flow region is large in extent, and covers about one third of the afterbody at all Mach numbers. The pressure distribution in the separated flow region exhibits a rise to separation, a plateau, and a recompression. These results are very similar to those obtained by Kuehn[2] for separation over forward facing flares. Even though large pressure gradients occur near the points of separation and reattachment, there exists an intermediate region, or plateau of nearly constant pressure very close to the freestream value at all three Mach numbers.

The 16° mean angle circular arc afterbody was used as a reference for examination of the effects of the ratio of approach boundary-layer displacement thickness to maximum afterbody radius, δ^*/R, and freestream total pressure, P_t, upon the onset and extent of separation. Figure 4 compares the pressure distribution over the model for two different boundary-layer thicknesses. The boundary-layer variations result in two opposing effects. First, a thicker, lower energy boundary-layer will tend to separate sooner for a given adverse pressure gradient. On the other hand, a thicker boundary-layer and accompanying separation region yield a greater displacement thickness effect which smooths out the effective contour encountered by the in-

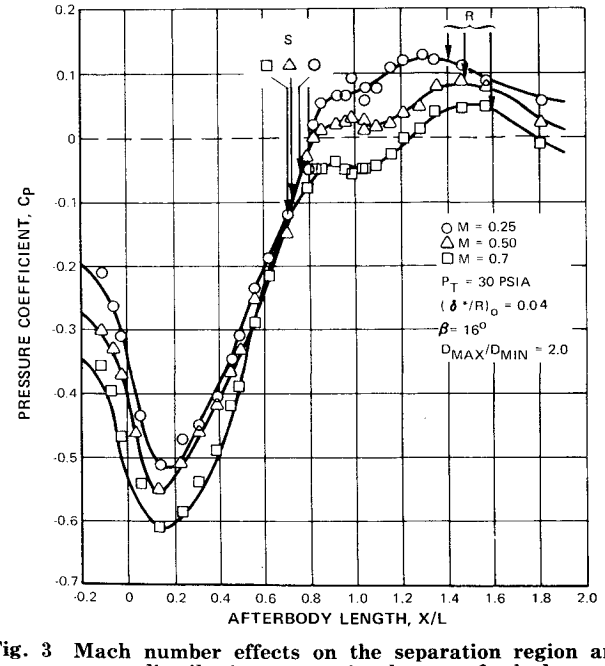

Fig. 3 Mach number effects on the separation region and pressure distribution over a circular arc afterbody.

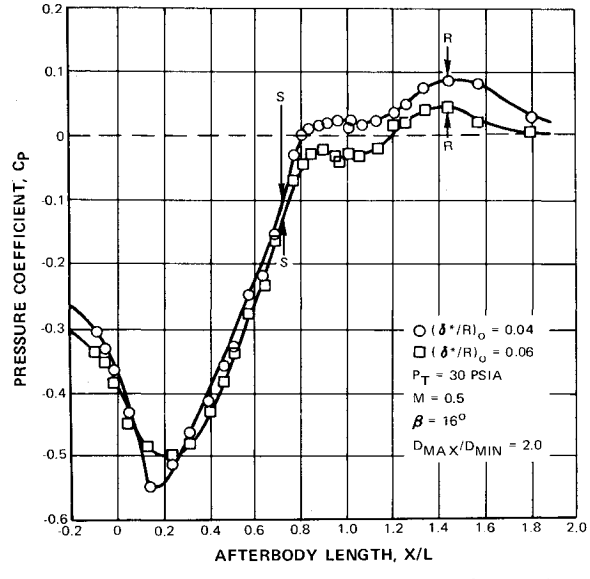

Fig. 4 Boundary-layer effects on the separation region and pressure distribution over a circular arc afterbody.

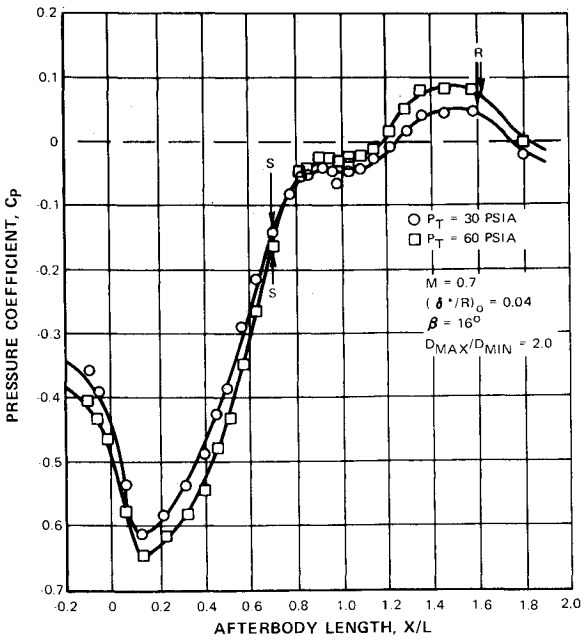

Fig. 5 Total pressure effects on the separation region and pressure distribution over a circular arc afterbody.

viscid flow thereby reducing the adverse pressure gradient. As a result of these two opposing effects the separation point tends to remain nearly fixed with variation in boundary-layer thickness as shown in Fig. 4. The reattachment point moves slightly downstream with increases in approach boundary-layer thickness. The movement is small and within the pressure-measurement system accuracy.

The effect of freestream total pressure at a freestream Mach number of 0.70 is shown in Fig. 5. The total pressure variation at constant Mach number may be interpreted as a Reynolds number variation. Again, the separation point remains nearly fixed with total pressure variations while the downstream reattachment point moves somewhat. It may be reasoned that the total pressure

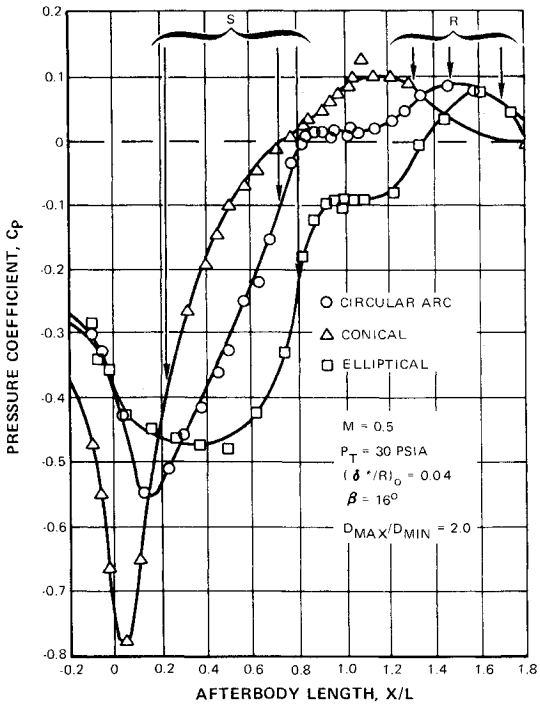

Fig. 6 Contour effects on the separation region and pressure distribution over an afterbody model.

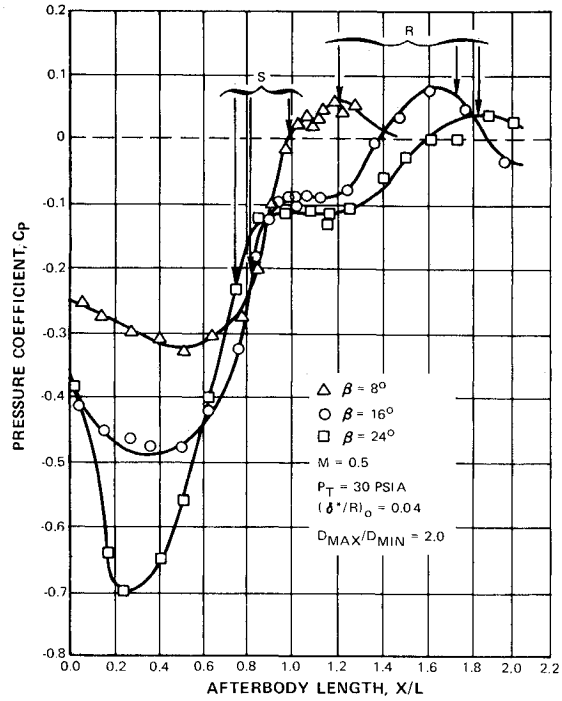

Fig. 7 Mean angle effects on the separation region and pressure distribution over an elliptical afterbody.

variation primarily affects boundary-layer thickness and this leads to the two opposing effects just discussed with little net change in the separation point location.

Figures 6–8 show how afterbody shape affects separation. Figure 6 presents the pressure distributions and the separation and reattachment points on three afterbody models having the same mean angle (16°) but different contours (conical, circular arc, and elliptical). The separation point is directly related to the pressure gradient pro-

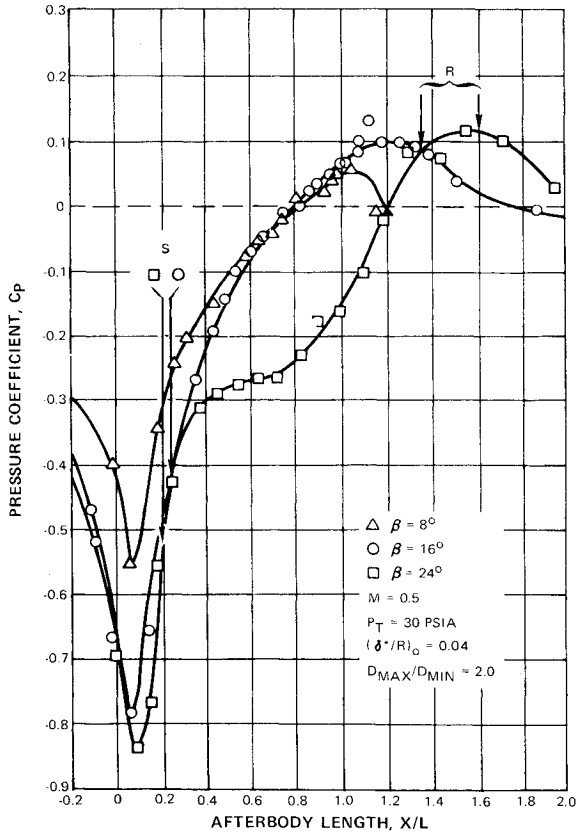

Fig. 8 Mean angle effects on the separation region and pressure distribution over a conical afterbody.

duced by the contour. The elliptical afterbody experiences the strongest recompression rate and the corresponding pressure rise from the minimum pressure point to separation is the lowest for this model. The circular arc afterbody which has a lower minimum pressure but also a less steep pressure rise, actually separates at a higher pressure and thus has a higher plateau pressure. The constant pressure plateau seen with both the elliptical and circular arc afterbodies reflects low velocities in a fairly thick recirculation region. No such plateau region is seen for the conical afterbody which has the longest separated region. The separation region on this model is very thin and its effect is similar to that of the displacement thickness of a normal boundary-layer. Apparently the contour is a major factor determining the pressure field over the separation region of an afterbody.

Figures 7 and 8 show the effects of mean angle on separation and pressure distribution for elliptical and conical afterbodies, respectively. The separation point moves upstream and the reattachment point moves downstream as the elliptical afterbody mean angle increases. The recompression pressure peaks would increase for attached flow as more and more expansion occurred on an afterbody. Separation eliminates this effect giving relatively the same recompression peak for all three models. The main difference observed with the conical afterbody (Fig. 8) is that the separation point remains near the corner which apparently tends to trigger separation for all mean angles. An increase in mean angle only moves the downstream reattachment point which in turn increases the recirculation region thickness. The effect of the downstream separation region thickening can be enough to give familiar plateau pressure distributions at very large angles as shown for the 24° case.

Comparison of Data with Theory

Presently available separation criteria are limited in scope and unproved for afterbody configurations mainly because they tend to oversimplify a complicated process which depends upon many parameters. Separation on afterbodies generally causes strong nonlinear interactions with the entire flowfield and is therefore not an isolated phenomenon. This interaction causes alteration of the upstream pressure distribution which in turn alters the turbulent boundary-layer development and the extent of the separated recirculation region. The problem is particularly severe at subsonic and transonic speeds where the downstream phenomena strongly influence the upstream conditions.

As mentioned in the last section, the pressure coefficient at separation is a function of Mach number, Reynolds number, contour shape, and boundary-layer history.[4-6] Few existing separation criteria take all of these factors into account and none consider the nonlinear interaction effects discussed above. These methods can then be properly used only with the aid of experimentally obtained pressure distributions. The pressure distribution and separation measurements given here do, however, form a consistent data set for determining the accuracy of existing separation prediction schemes subject to these limitations. The following commonly used separation criteria will therefore be compared to the data:

Shape Factor Criterion[7]

This criterion is based on the solution of the momentum integral equation for boundary-layer flow using modified equations of Reshotko and Tucker.[8] An approximate shear integral obtained by a correlation of extensive data in an adverse pressure gradient is used. A shape factor of $H = \delta^*/\Theta = 1.75$ is taken to indicate flow separation.

Stratford Criterion[9]

This approach is based on an approximate solution of the equations of motion; a single empirical factor is required. The equations are integrated using a modified inner and outer solution technique. It is assumed that the outer part of the boundary layer is affected only by the initial velocity profile and the downstream pressure gradient, and the inner part of the boundary layer is locally in equilibrium and is independent of upstream conditions. At Reynolds number of order 10^6 the criterion is:

$$C_{ps}(xdC_{ps}/dx)^{1/2} = 0.98\,(Re_x)^{1/10}$$

The distance x represents an equivalent length of flat-plate, constant-pressure boundary-layer growth. Re_x is the Reynolds number based on this equivalent length. The subscript s is used to reference the required pressure for separation.

Page Criterion[10]

This is probably the most commonly referenced approach for prediction of the local separation point. The recirculation region is modeled as a base-type region and entrainment equations for constant pressure viscous mixing are used to derive an equilibrium pressure. In its original form for subsonic flow the criterion is $C_s = 0.38$ where C_s is a modified separation pressure coefficient defined as

$$C_s = (2(P_s - P_\infty)/kP_sM_s^2)$$

Eilers[11] modified this criterion for use on axisymmetric afterbodies where the boundary layer goes through a strong expansion before recompressing through a separated region. This modified version, which will be used herein, is $C_s = C_m + 0.38$, where C_m is defined as

$$C_m = (2(P_m - P_\infty)/kP_mM_m^2)$$

The subscript m indicates reference to the point of minimum pressure on the afterbody.

Goldschmied Criterion[12]

This criterion was originally derived for planar incompressible flow. The criterion is based on a line of constant total pressure occurring in a boundary layer, even under an adverse pressure gradient. At separation the height of the constant pressure line and the laminar sublayer are equal. The resulting criterion becomes $C_{ps} = 200\ C_{fm}$ where C_{fm} is the skin friction coefficient at the minimum pressure point on the afterbody. This separation prediction technique is independent of the pressure distribution downstream of the minimum pressure point and is dependent on Reynolds number and Mach number only through the skin friction coefficient.

Control Volume Criterion[3]

A control volume in the boundary layer between the minimum pressure point and the point of separation on the afterbody is used. Conservation of mass and momentum through the volume, along with the compressible law of the wall law of the wake[13] boundary-layer profiles are used to calculate the separation pressure. This approach has been used extensively for shock-induced separation.

Figures 9 and 10 show a comparison of these criteria when applied to the pressure data measured on two afterbody models at Mach numbers 0.25 and 0.50. Figure 9 presents results for the circular arc afterbody with a 16° mean angle at $M = 0.5$. The shape factor and Goldschmied criteria predict no separation while the Stratford and Page criteria predict separation on the downstream sting. The only criterion that reasonably predicts the point of separation on this model is the control volume

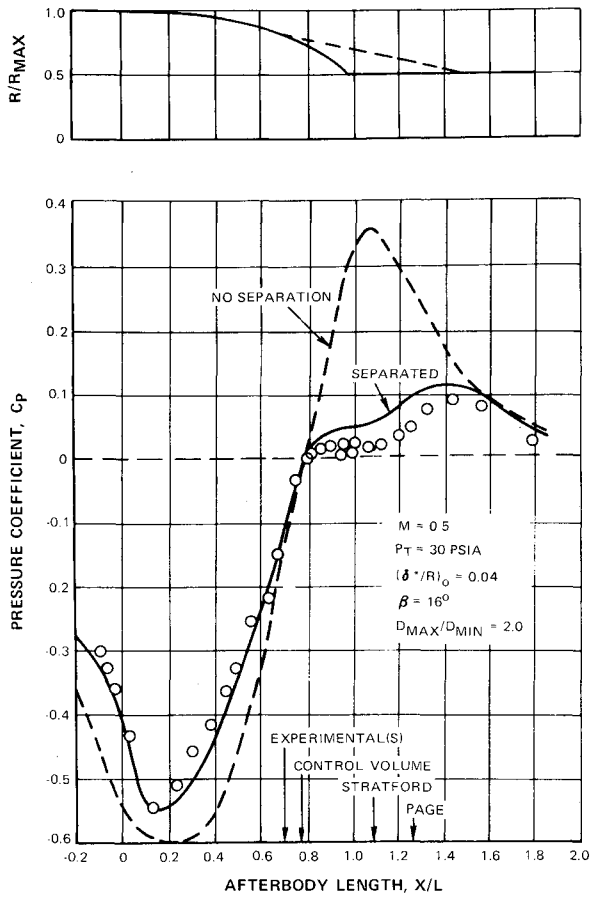

Fig. 9 Experimental and calculated pressure distribution and separation points over a separated circular arc afterbody model.

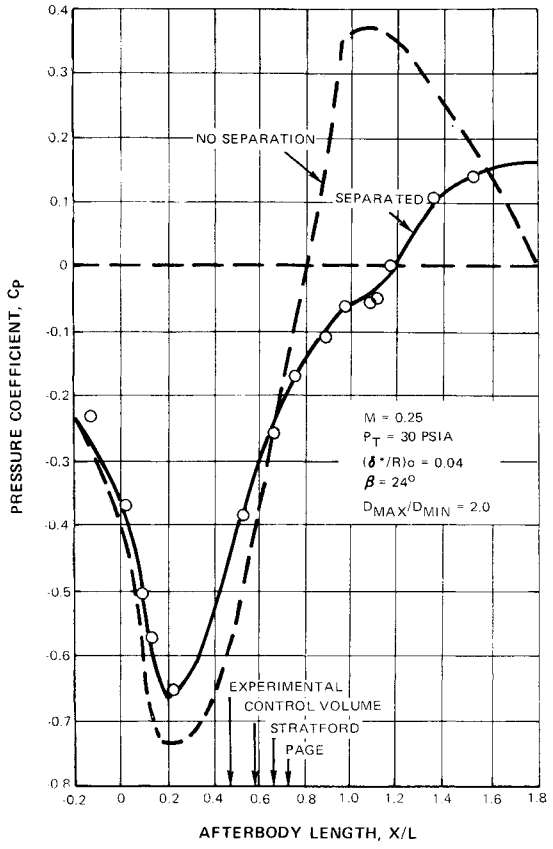

Fig. 10 Experimental and calculated pressure distributions over a separated elliptical afterbody model.

approach. Similar results are presented in Fig. 10 for an elliptical afterbody at $M = 0.25$.

The curves shown in Figs. 9 and 10 represent the pressure distributions over the models calculated from potential flow theory[14] modified with Gothert's compressibility correction[15] and coupled to a boundary-layer calculation.[8] The dashed curve was obtained with the inviscid calculation neglecting separation effects but including tunnel-wall influence. This approach greatly over estimates the flow perturbations occurring on the afterbody. It can be seen that the separation causes a net decrease and leveling off of the recompression pressure peak predicted by the inviscid analysis. The solid curve represents the inviscid pressure distribution obtained with a conical discriminating streamline surface between the experimentally measured point of separation and reattachment. The pressures obtained using this approach agree surprisingly well with data.

The corresponding calculated and measured drag variations with mean angle over the elliptical models, are shown in Fig. 11 in terms of drag coefficients, C_d, based on maximum afterbody area. The potential flow calculation without separation predicts very little drag; much less than what was measured on the models. The high recompression pressure prediction on the rearward portion of the afterbody as shown previously in Fig. 10 produces a thrust force which very nearly counterbalances the drag force due to the expansion region. However, this high recompression pressure never appears when separation occurs, rather, the pressures level off and afterbody drag increases drastically.

Figure 11 also shows how one may use the conical dividing streamline to predict the effect of separation on the inviscid flowfield. A drag variation with mean angle is calculated using this approach that agrees quite well with the data in both magnitude and shape. The simple conical dividing streamline model for the recirculating region can then be very useful when calculating the pressure and drag over a separated afterbody because it gives a first-order effect of the recirculating flow. In Ref. 3 this approach is pursued much further with reasonable success.

Conclusions

The results of this experimental program suggests the following conclusions about separation over an axisymmetric afterbody.

1) Separation can drastically affect the pressure distribution over an entire afterbody; thus the inviscid pressure

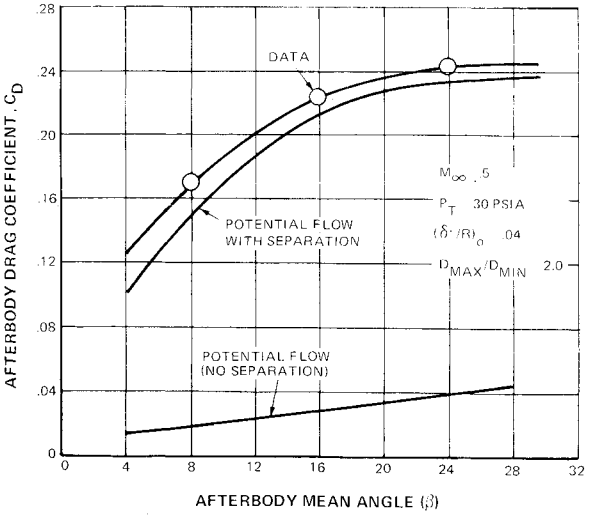

Fig. 11 Afterbody drag variation with mean angle for elliptical afterbodies.

distribution of the model is seldom a good first-order approximation.

2) The pressure distribution on a steep afterbody exhibits a plateau pressure region near freestream pressure when the recirculation region is of considerable extent and depth.

3) The length of the separation region seems to be a function of Mach number, with larger regions and earlier separation occurring at high Mach numbers.

4) The point of separation on an afterbody cannot accurately be determined from the pressure distribution alone.

5) Large discrepancies exist between existing separation criteria and the data.

6) The separated region can be modeled fairly well by a conical dividing streamline surface between the point of separation and the point of reattachment. The inviscid pressure distribution over the body including this dividing streamline seems to be a good first-order approximation to the actual separated pressure field.

References

[1]Chang, R. K., *Separation of Flow*, Pergamon Press, New York, 1970, pp. 1-200.

[2]Kuehn, D. M., "Experimental Investigation of the Pressure Rise Required for the Incipient Separation of Turbulent Boundary Layers in Two-Dimensional Supersonic Flow," Memo 1-21-59A, 1959, NASA.

[3]Presz, W. M., Jr., "Turbulent Boundary Layer Separation on Axisymmetric Afterbodies," Ph.D. thesis, 1974, School of Engineering, Univ. of Connecticut, Storrs, Conn.

[4]Hahn, M., Rubbert, P., and Mahal, A., "Evaluation of Separation Criteria and Their Application to Separated Flow Analyses," AFFDL-TR-72-145, 1973, Air Force Flight Dynamics Lab., Wright-Patterson Air Force Base, Ohio.

[5]Stanewsky, E. and Little, B. H., "Separation and Reattachment in Transonic Airflow," *Journal of Aircraft*, Vol. 8, No. 12, Dec. 1971, pp. 952-960.

[6]Cebeci, T., Mosinski, G. J., and Smith, A. M. O., "Calculation of Separation Points in Incompressible Turbulent Flows," *Journal of Aircraft*, Vol. 9, No. 9, Sept. 1972, pp. 618-624.

[7]Reshotko, E. and Tucker, M., "Approximate Calculation of the Compressible Turbulent Boundary Layer with Heat Transfer and Arbitrary Pressure Gradient," TN-4154, 1957, NASA.

[8]Elliot, D. G., Bartz, D. R., and Silber, S., "Calculation of Turbulent Boundary Layer Growth and Heat Transfer in Axisymmetric Nozzles," TR-32-387, 1963, Jet Propulsion Lab., Pasedena, Calif.

[9]Stratford, B. S., "The Prediction of the Turbulent Boundary Layer," *Journal of Fluid Mechanics*, Vol. 5, 1959, pp. 1-16.

[10]Page, R. H., "A Theory for Incipient Separation," in *Developments in Mechanics*, Vol. 1, Plenum Press, New York, 1961, pp. 563-577.

[11]Eilers, R. E., "Analytical Investigation of Subsonic Separation from Axisymmetric Boattails," D6-20399, A68, 1968, Boeing Aircraft Co., Seattle, Wash.

[12]Goldschmied, F. R., "An Approach to Turbulent Incompressible Separation Under Adverse Pressure Gradients," *Journal of Aircraft*, Vol. 2, No. 2, March-April 1965, pp. 108-115.

[13]Mathews, D. C., Paynter, G. C., and Childs, M. E., "Use of Coles' Universal Wake Function for Compressible Turbulent Boundary Layers," *Journal of Aircraft*, Vol. 7, No. 2, March-April 1970, pp. 137-140.

[14]Smith, A. M. O. and Pierce, J., "Exact Solution of the Nuemann Problem; Calculation of Non-Circulatory Plane and Axial Symmetry Flow About or Within Arbitrary Boundaries," *Proceedings of the Third U.S. National Congress of Applied Mechanics*, Vol. 2, 1968, Brown University, Providence, R.I., pp. 807-815.

[15]Shapiro, A. H., *The Dynamics and Thermodynamics of Compressible Fluid Flow*, Vol. 1, Ronald Press, New York, 1953, pp. 303-426

Airfoil Design for High Tip Speed Compressors

G. David Huffman*
Indianapolis Center for Advanced Research and Indiana-Purdue University at Indianapolis, Ind.
and
P. C. Tramm†
Detroit Diesel Allison Division of General Motors, Indianapolis, Ind.

An investigation into the use of new airfoil designs to improve the efficiency of high tip speed fans and multistage compressors is in process. Two-dimensional cascade test data are presented for a conventional multiple circular arc airfoil design and for one designed to an unstarted strong oblique shock wave pattern. Both airfoils have a 1.588 design point inlet Mach number. Design flow conditions are generally achieved; the multiple circular arc airfoil has better performance at low pressure ratios and the airfoil using an unstarted strong oblique shock system is superior at high pressure ratios. A categorization of the losses is presented.

Presented as Paper 73-1248 at the AIAA/SAE 9th Propulsion Conference, Las Vegas, Nev., November 5-7, 1973; submitted February 21, 1974; revision received August 16, 1974. This work was carried out as one phase of the U.S. Air Force Turbine Engine/High Flow Compressor Program.[1]

Index categories: Airbreathing Propulsion, Subsonic and Supersonic; Subsonic and Transonic Flow.

*Center Fellow and Professor of Engineering and Adjunct Professor of Mathematical Sciences; formerly Chief, Mechanics Research, Detroit Diesel Allison. Associate Fellow AIAA.

†Chief, Internal, Aerodynamics Research. Member AIAA.

Nomenclature

A = area, in.^{2} (m^2)
c = airfoil chord, in. (mm)
C_p = static pressure coefficient, $[2(p - p_1)]/[k\, p_1\, M_1^2]$
D = diffusion factor, $1 - V_2/V_1 + \sin(\beta_2)[1 - V_{y2}/V_{y1}]/2\sigma$
k = ratio of specific heats
l = distance along the chord line from the leading edge, in. (mm)
M = Mach number
p = static pressure, lb$_f$/in.^{2} (pa)
P = total pressure, lb$_f$/in.^{2} (pa)
r = radius, in. (mm)